^{13}C and ^{31}P NMR Study of Gluconeogenesis: Utilization of ^{13}C-Labeled Substrates by Perfused Liver from Streptozotocin-Diabetic and Untreated Rats

Sheila M. Cohen

Department of Biophysics, Merck Institute for Therapeutic Research, Merck Sharp & Dohme Research Laboratories, Rahway, New Jersey 07065

Received March 17, 1986; Revised Manuscript Received September 25, 1986

ABSTRACT: The metabolism of ^{13}C-labeled substrates was followed by ^{13}C and ^{31}P NMR in perfused liver from the streptozotocin-treated rat model of insulin-dependent diabetes. Comparison was made with perfused liver from untreated littermates, fasted either 24 or 12 h. The major routes of pyruvate metabolism were followed by a ^{13}C NMR approach that provided for the determination of the metabolic fate of several substances simultaneously. The rate of gluconeogenesis was 2–4-fold greater and β-hydroxybutyrate production was 50% greater in liver from the chronically diabetic rats as compared with the control groups. Large differences in the distribution of ^{13}C label in hepatic alanine were measured between diabetic and control groups. The biosyntheses of ^{13}C-labeled glutathione and *N*-carbamoylaspartate were monitored in time-resolved ^{13}C NMR spectra of perfused liver. Assignments for the resonances of glutathione and *N*-carbamoylaspartate were made with the aid of ^{13}C NMR studies of perchloric acid extracts of the freeze-clamped livers. ^{13}C NMR spectroscopy of the perfusates provided a convenient, rapid assay of the rate of oxidation of [2-^{13}C]ethanol, the hepatic output of [2-^{13}C]acetaldehyde, and the accumulation of [2-^{13}C]acetate in the perfusate. By ^{31}P NMR spectroscopy, carbamoyl phosphate was measured in all diabetic livers and an unusual P,P′-diesterified pyrophosphate was observed in one-fourth of the diabetic livers examined. Neither of these phosphorylated metabolites was detected in control liver. Both ^{13}C and ^{31}P NMR were useful in defining changes in hepatic metabolism in experimental diabetes.

The chief precursors of gluconeogenesis in vivo—alanine and lactate—enter the pathway as pyruvate. The three enzymes catalyzing the major routes of pyruvate metabolism in liver have been demonstrated to be important in the regulation of gluconeogenesis. Two of these enzymes, pyruvate carboxylase and pyruvate kinase, have been implicated in the hormonal control of glucose synthesis from substrates that enter the pathway at the level of pyruvate (Kraus-Friedmann, 1984). Because the third enzyme, pyruvate dehydrogenase, competes with pyruvate carboxylase for entry of pyruvate into the tricarboxylic acid (TCA) cycle, its regulation is also relevant to the control of gluconeogenesis.

This study focuses on the use of ^{13}C NMR spectroscopy to investigate the pathway from either [3-^{13}C]alanine or [2-^{13}C]pyruvate + NH_4Cl into glucose in perfused liver from normal control rats and from the streptozotocin-treated rat model of insulin dependent diabetes. Observations made in this study correlate with and provide a foundation for specific ^{13}C NMR assays of relative fluxes through the major enzymes of pyruvate metabolism. These assays are described in two companion papers (Cohen, 1987a,b). In the first paper, a ^{13}C NMR determination of the activity of the phosphoenolpyruvate (PEP) cycle in perfused liver is developed, and the effect of insulin in vitro on the activity of this cycle in liver from diabetic and fasted normal control rats is tested (Cohen, 1987a). This assay utilizes differences in ^{13}C enrichment at the randomized carbons of alanine observed here between diabetic and control liver. In the second paper, the relative proportions of pyruvate entering the TCA cycle by the competing routes through pyruvate carboxylase and pyruvate dehydrogenase are estimated from the ^{13}C enrichments in the individual carbons of glutamate (Cohen, 1987b). The fluxes measured through these competing routes generally correlate with the higher rates of gluconeogenesis measured here in liver from diabetic or fasted control rats and are consistent with our observations of the biosynthesis of ^{13}C-labeled fatty acids in liver from fed (Cohen, 1987b) or 12-h-fasted control rats but not from either diabetic or 24-h-fasted control rats.

To enhance the ability of ^{13}C NMR to measure a number of metabolites simultaneously in a single spectrum, livers were perfused with two different specifically labeled gluconeogenic substrates. [2-^{13}C]Pyruvate or [3-^{13}C]alanine, usually in the presence of labeled ethanol, is used here. These substrates allow us to build upon the background provided by previous studies (Cohen et al., 1981a; Cohen, 1983). Other reasons for using these combinations of substrates include such considerations as follows: (a) Introduction of ^{13}C–^{13}C *J* splitting to aid in the identification of metabolites and in the tracing of metabolic pathways. The assignment of the resonances of glutathione was aided by this device in this study. (b) Provision of redundancy for checking the reliability of measured parameters, such as Nuclear Overhauser Effect (NOE) values, as applied to perfused liver. (c) Provision of flexibility in experimental design so that the specific label best suited to a given task can be used. As an example, [3-^{13}C]alanine is the preferred substrate for assays that depend upon the relative enrichment in glutamate because this flow of label can be measured with greater accuracy under our conditions than that from [2-^{13}C]pyruvate. (d) Addition of ^{13}C-labeled ethanol along with labeled alanine or pyruvate in this study allowing the development of a rapid ^{13}C NMR assay of the hepatic rate of oxidation of ethanol and the accumulation of acetate and acetaldehyde in the perfusate. While use of substrate combinations does increase the complexity of the resulting spectra, there is a roughly corresponding increase in the information available. This approach may be useful in the design of in vivo studies by suggesting guidelines for obtaining a maximum of information from one time sequential series of ^{13}C NMR spectra.

Because ^{13}C and ^{31}P nuclei frequently give complementary information, the acquisition of both ^{13}C and ^{31}P NMR spectra of the same, isolated perfused rat liver can give a fairly com-

0006-2960/87/0426-0563$01.50/0

prehensive view of the regulation of hepatic metabolism (Cohen, 1983). In this study, carbamoyl phosphate was measured in all diabetic livers, and an unusual P,P′-diesterified pyrophosphate was observed in 25% of the diabetic livers examined by ^{31}P NMR spectroscopy. Neither of these metabolites was detected in any control liver by ^{31}P NMR.

Materials and Methods

Animals. Diabetes was produced in female Fischer-344 rats (Charles River Breeding Laboratories), with initial body weights of 125–150 g, by intravenous injection of streptozotocin at a dose of 45 mg/kg of body weight. Treated rats showed little or no weight gain and had plasma glucose levels in excess of 300 mg/100 mL and were, hence, considered to be diabetic. These rats were maintained for 1 month to allow stabilization of the diabetic condition. Both diabetic rats and their untreated littermates were fed Purina Chow ad libitum. Control rats were divided into two groups: one group was fasted for 24 h before the start of the perfusion experiment; the second group was fasted for 12 h. Diabetic rats were not fasted. Rats were about 12 weeks of age at the time of the perfusion. All animals had free access to water at all times. The animals were anesthetized with sodium pentobarbital (50 mg/kg).

Sample Preparation for NMR Studies. The isolated rat liver perfusion technique, as modified for NMR studies, has been described in detail previously. As before, during the initial 30–40-min period of perfusion, the perfusate was not recirculated. The purpose of this period of substrate-free flow-through perfusion was to wash out and deplete remaining endogenous substrates. After this period, the perfusate was exchanged for one containing fresh, washed dog erythrocytes suspended to a hematocrit of 27% in Krebs' bicarbonate buffer (Cohen, 1983).

NMR Conditions. NMR spectra were measured at 8.46 T on a Bruker WH360 wide-bore spectrometer operating in the Fourier-transform mode. Conditions were generally as described before (Cohen, 1983). However, in this study two selectively tuned probes were used; one probe was tuned to the ^{13}C frequency, 90.5 MHz, and the other to the ^{31}P frequency, 145.8 MHz. Both probes had main coils of the Helmholtz type and accommodated 20-mm NMR tubes.

Spectra of perfused liver were measured at 35 ± 1 °C. Accumulation of NMR data began with the recirculation of the perfusate containing erythrocytes. For each liver, the following protocol was followed: (a) Two ^{31}P NMR spectra were accumulated first to assess the viability of the preparation. Each spectrum consisted of 400 scans of 30° free-induction decays (FIDs) with a 12-kHz window. Six minutes of data accumulation was required. No exogenous substrate was present at this time. (b) A series of ^{13}C NMR spectra was accumulated after the spectrometer was converted to ^{13}C conditions (about 8-min elapsed time for the conversion). For each liver, one ^{13}C spectrum was accumulated before the addition of substrate. For ease of interpretation, this ^{13}C natural abundance background spectrum of a given liver was subtracted in the computer from each spectrum accumulated after the addition of ^{13}C-labeled substrate before hard copies of the spectra were made. All ^{13}C spectra were broad-band ^{1}H decoupled. Each ^{13}C spectrum required 10.7-min data accumulation and consisted of 800 scans, with 0.8-s recovery between 30° FIDs. (c) After the accumulation of the ^{13}C NMR spectra, spectrometer conditions were reverted to those for the ^{31}P nucleus, and typically, two final ^{31}P NMR spectra were accumulated. (d) At the termination of the perfusion, the liver was freeze-clamped and stored at −70 °C until a perchloric acid extract was prepared, as described previously (Cohen, 1983). (e) The erythrocytes were then removed from the perfusate by centrifugation, and the resulting cell-free perfusate was stored at −70 °C until needed.

Certain spectra, viz., those of perfusates or perchloric acid extracts, were acquired under other conditions, which are specified in the figures. NMR conditions for perfused liver were selected to optimize signal-to-noise with minimum distortion of intensities, whereas conditions for perfusates and extracts were those determined to be essentially nonsaturating. In a manner similar to that described before (Cohen, 1983), optimized NMR conditions were determined for the selective ^{13}C probe for natural abundance glucose, amino acids, Krebs cycle intermediates, and ketone bodies in three model solutions designed to simulate the salt conditions and pH of (1) perfusates, (2) perchloric acid extracts, and (3) liver. Nuclear Overhauser effect (NOE) values were determined by a standard method (Canet, 1976). However, because this study emphasizes the use of relative ^{13}C enrichments at various carbons of a given metabolite, our main approach has been to measure the relevant intensity ratios under the exact conditions used in the corresponding metabolic study. Under ideal conditions, the ratios of the integrated intensities for the natural abundance compounds would be expected to be 1.0; thus, the measured ratios take into account differences in both relative saturation and NOE values. Under the conditions used here, in model solution 2 (extract conditions), the intensity ratios of glutamate C-2/C-3 and C-4/C-3 were 1.00 ± 0.02, that of aspartate C-2/C-3 was 0.98, that of *N*-carbamoylaspartate C-2/C-3 was 1.04, and that of alanine C-2/C-3 was 1.01. In model solution 3 (liver NMR conditions), the intensity ratio of glutamate C-2/C-3 was 0.79 and C-4/C-3 was 0.86, that of aspartate C-2/C-3 was 0.87, that of alanine C-2/C-3 was 0.71, and that of lactate C-2/C-3 was 0.64. In model solution 1 (perfusate NMR conditions), all intensity ratios for carbons 2, 3, and, where applicable, 4 of glutamate, aspartate, alanine, lactate, and β-hydroxybutyrate were 1.00 ± 0.04; all possible ratios of the carbons of glucose were 1.00 ± 0.04. The expected errors for label distribtions measured in ^{13}C NMR studies of hepatic metabolism range from ±2 to ±7% (Cohen et al., 1981b). While the intensity ratios measured in spectra of perfused liver must be corrected for the differences noted above, these results indicate insufficient justification for correction of the ratios measured in perfusates or extracts under our conditions. To estimate absolute concentrations of certain metabolites present in the perfusates from the intensities of their NMR signals relative to the area of the glucose C-6 signal, it was necessary to measure (a) all relevant NOE values, (b) the concentration of glucose by a standard chemical method, and (c) the ^{13}C enrichment of C-6 of glucose. The NOE values of the various carbons present in two model perfusate solutions, A and B, were measured by a standard method (Canet, 1976). Model solution A contained unlabeled glucose, β-hydroxybutyrate, ethanol, acetate, and lactate. Model solution B contained unlabeled glucose, alanine, and acetaldehyde. The NOE of glucose C-6 was greater than that of the NOE of any other carbon of interest. The factor by which the area of a given peak must be multiplied to estimate that carbon's concentration relative to the concentration of glucose C6 in the perfusates is as follows: β-hydroxybutyrate C-2 by 1.49, C-3 by 1.53, and C-4 by 1.51; ethanol C-2 by 1.77; acetate C-2 by 2.43; lactate C-2 by 1.81 and C-3 by 1.50; alanine C-3 by 1.38; acetaldehyde C-2 by 1.40.

^{13}C chemical shifts are given relative to tetramethylsilane at 0 ppm. ^{31}P chemical shifts are given relative to *sn*-glycero-3-phosphocholine (GPC) at 0.494 ppm (equivalent to

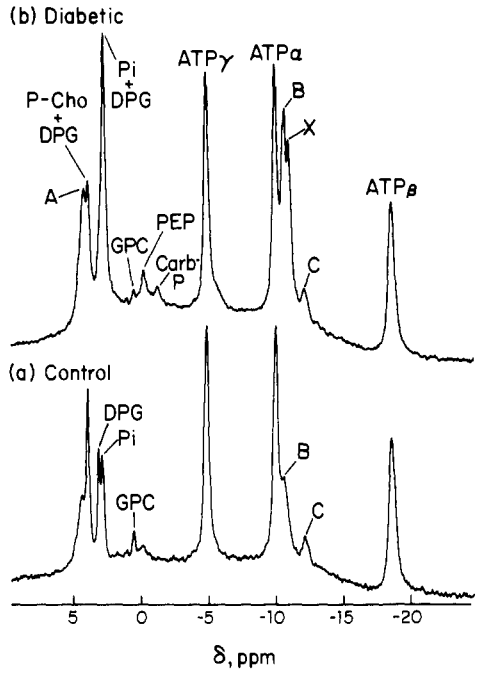

FIGURE 1: ^{31}P NMR spectra of isolated perfused rat liver from (a) 24-h-fasted control rat and (b) diabetic rat at 35 ± 1 °C. Each spectrum was measured 216–222-min postsubstrate and 16 min after the final ^{13}C NMR spectrum was accumulated in the respective perfusions. Each spectrum is the Fourier transform of 400 free induction decays. The labeled ^{31}P NMR peaks include the following: P-Cho, P-choline; P_i, inorganic orthophosphate; GPC, *sn*-glycero-3-phosphocholine; PEP, P-enolpyruvate; Carb-P, carbamoyl-P. Region A includes sugar phosphates, AMP, and 3-P-glycerate. Peak B includes the dinucleotides, predominantly NAD^+. Peak X is an unknown P,P′-diesterified pyrophosphate, and peak C includes the nucleoside diphosphosugars. The peaks labeled DPG are due to D-glycerate-2,3-P_2 in the fresh, washed erythrocytes of the perfusate.

85% orthophosphoric acid at 0 ppm). The IUPAC convention for the chemical shift scale is used. Identification of the NMR peaks has been described before (Cohen et al., 1981b). Identifications of certain metabolites, viz., glutathione and *N*-carbamoyl-L-aspartate, which had not been observed in previous work, were based on standard approaches, including comparison of chemical shifts and ^1H–^{13}C coupling constants with those of the authentic compounds under the same conditions, comparison of the dependence of the chemical shift upon pH for the unknown and the authentic compound, and, sometimes, observation of whether the addition of a small amount of the authentic compound to the extract increased the intensity of the unknown peak.

[3-^{13}C]Alanine, [2-^{13}C]pyruvate, [2-^{13}C]ethanol, and [1,2-^{13}C]ethanol, (90% isotropic purity) were from Merck & Co., Inc./Isotopes (St. Louis, MO). Crystalline insulin (from bovine pancreas) and bovine serum albumin (essentially fatty acid free, fraction V) were from Sigma. Other chemicals were of the highest purity obtainable. Glucose was assayed in aliquots of perfusate by the hexokinase method with a Rotochem IIa analyzer.

Results

Effects of Diabetes on Phosphate Metabolites As Studied by ^{31}P NMR. Figure 1a shows a typical ^{31}P NMR spectrum of liver from an untreated control rat after a total perfusion time of 4.6 h. ATP and intracellular P_i were approximately constant during this period. Under the same perfusion conditions, ATP levels in diabetic liver show a small decline after 4.6 h of perfusion, independent of the presence of insulin (Figure 1b). The level of P_i in the diabetic liver was signif-

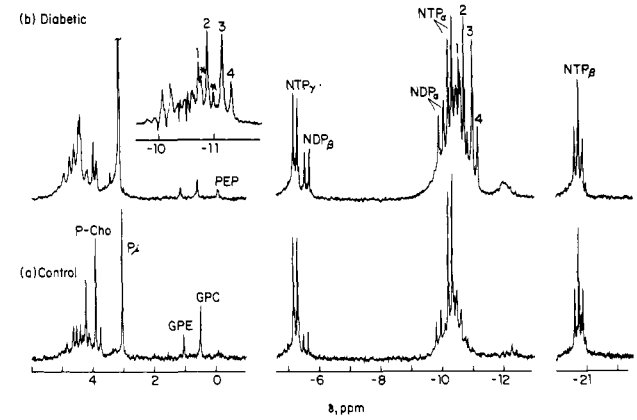

FIGURE 2: ^{31}P NMR spectra of perchloric acid extracts of freeze-clamped liver from (a) control rat and (b) diabetic rat at 12 °C. Shortly after the spectrum shown in Figure 1*a* was recorded, the liver was freeze-clamped and the extract shown in spectrum a was prepared. Spectrum a is the Fourier transform of 10 800 pulses of 45° free-induction decays, with 1.64-s recovery time between pulses. Spectrum b shows the extract of the diabetic liver of Figure 1b; this liver and its extract were treated exactly the same as the control liver and its extract. Both extracts were at pH 8.2. The abbreviations used are given in Figure 1 with the following exceptions: NTP, nucleoside triphosphate; NDP, nucleoside diphosphate; GPE, *sn*-glycero-3-phosphoethanolamine. The peaks labeled 1–4 and by the asterisks are described in the text. The insert shows an expansion of the −10 to −12 ppm region of the difference spectrum of spectrum b minus spectrum a.

icantly higher than the level measured in the control, both at the beginning and at the end of the perfusion period. Two major differences between the two spectra shown in Figure 1 are apparent. First, under the same conditions and with the same substrate, [3-^{13}C]alanine and [2-^{13}C]ethanol, carbamoyl phosphate is detectable in the diabetic liver but not in the control. Second, a new signal, labeled X in Figure 1b, appears in the diabetic liver but not in the control. Peak X is in the P,P′-diesterified pyrophosphate region and was present at detectable levels in 25% of the diabetic livers examined (n = 16); this signal was not detectable in any control liver studied (n = 15).

^{31}P NMR spectra (Figure 2) of the perchloric acid extracts of these two livers provide considerable additional information. Assignments such as those of GPC and PEP are confirmed, and it is seen that the peaks labeled ATPγ, ATPα, and ATPβ for convenience in Figure 1 are actually composed of both purine and pyrimidine nucleoside di- and triphosphates. In Figure 2, the pyrimidine nucleoside triphosphates can be seen most easily as low-intensity peaks, slightly upfield of the corresponding purine peaks at NTPβ. The ratio of pyrimidine to purine nucleoside triphosphates in livers from two diabetic and two control rats was 0.30 ± 0.05, as estimated from peak heights in ^{31}P spectra of the extracts after application of a convolution difference technique. Whereas the ratio of NTP/NDP in the control liver shown in Figure 1a is about 9:1, this ratio in the extract (Figure 2a) is only 5:1. The corresponding NTP/NDP ratios for the diabetic liver in these figures are 7.5:1 and 2.4:1, respectively. Much of this difference arises because ^{31}P NMR spectra of perfused liver measure free, presumably cytosolic, concentrations of ATP and ADP, whereas spectra of extracts measure the total liver ATP and ADP content, including mitochondrial ADP that had existed in a tightly bound state in the intact cell. The NTP/NDP ratios measured here in liver and extracts, from either control or diabetic liver, fall within the range measured chemically for cytosol and whole liver, respectively (Schwenke et al., 1981).

The peak labeled X in Figure 1b was acid-extractable and appears as a quartet (peaks 1–4) in Figure 2b. In the conventional notation used for systems of magnetic nuclei occurring in molecules (Pople et al., 1959), a P,P′-diesterified pyrophosphate would be expected to give an AB quartet when observed with the high resolution obtainable in spectra of extracts. Peaks 1–4 in Figure 2b give a classic AB quartet with $J/\nu_0\delta = 0.4$, where J is the ^{31}P–^{31}P scalar coupling between the two phosphates, A and B, and $\nu_0\delta$ is the chemical shift difference between then in hertz. The J coupling for the quartet of Figure 2b is 23.8 Hz. The positions of the peaks labeled 1–4 of Figure 2b are −10.667, −10.830, −11.116, and −11.280 ppm, respectively. These positions are to be compared with those measured for the quartet given by NAD^+ in spectra of extracts of control liver; the positions of the corresponding NAD^+ peaks are −10.585, −10.728, −10.938, and −11.080 ppm. The two peaks labeled with an asterisk in the insert of Figure 2b are at −10.713 and −10.934 ppm, respectively, and thus are tentatively assigned to the two most intense signals of the NAD^+ quartet in this extract. The unknown P,P′-diesterified pyrophosphate can be distinguished on the basis of both chemical shifts and J coupling constant from the familiar compounds of this type, such as NAD^+, $NADP^+$, FAD, acetyl-CoA, coenzyme A, UDP-glucose, UDP-glucuronic acid, GDP-mannose, cytidine 5′-diphosphocholine, cytidine 5′-diphosphoethanolamine, and UDP-xylose, which are known to exist in liver. Not only are the chemical shifts of these compounds different from those of the unknown metabolite, but their J coupling constants are all in the range of 19–21 Hz, which is appreciably lower than the 23.8 Hz measured for the unknown. In addition to the 11 compounds named, 6 other commercially available compounds of this general type have been examined with the same negative result. These compounds include cytidine 5′-diphosphoglycerol, ADP-ribose, α-NAD^+, UDP-*N*-acetylglucosamine, nicotinamide hypoxanthine dinucleotide, and nicotinamide 1,N^6-ethenoadenine dinucleotide. Thus, further characterization of the unknown metabolite will require its isolation from the extracts by procedures that are outside the scope of this study.

The other major difference between the ^{31}P NMR spectra of diabetic (Figure 1b) and control (Figure 1a) liver is the appearance of carbamoyl phosphate (carbamoyl-P) in the former. With either [3-^{13}C]alanine or [2-^{13}C]pyruvate + NH_4Cl as substrate, carbamoyl-P rose to detectable levels in all diabetic livers studied. Under the same conditions, no signal for carbamoyl-P was detectable in any control liver. Because carbamoyl-P had disappeared by the time the liver shown in Figure 1b was freeze-clamped, another liver preparation from another diabetic rat was perfused under almost the same conditions. However, in this perfusion only ^{31}P data were accumulated so that the liver could be freeze-clamped when carbamoyl-P levels were elevated. In the presence of only lactate, no carbamoyl-P is seen (Figure 3a). Shortly after the addition of pyruvate, NH_4Cl, and ethanol, a pronounced signal for carbamoyl-P appeared (Figure 3b). PEP and 3-phosphoglycerate also increased, while P_i decreased sharply. If the assumption is made that the ATP level in this liver was about 3 mM, then the liver concentration of carbamoyl-P increased to about 0.4 mM. The assignment of carbamoyl-P was confirmed in the ^{31}P NMR spectrum of the extract (Figure 4) by comparison of the pH dependence of its chemical shift with that of authentic carbamoyl-P and by addition of a small amount of the authentic compound to the extract. The chemical shift of carbamoyl-P in spectra of diabetic liver (Figures 1b and 3b) is about −1.30 ppm. In metal-free

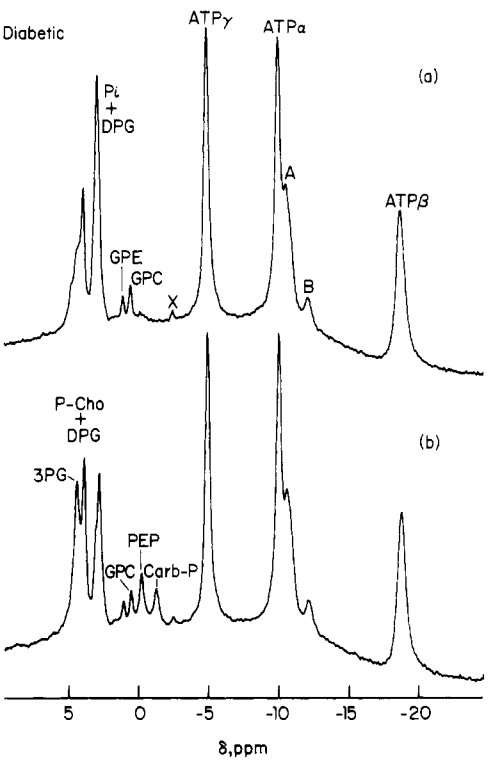

FIGURE 3: ^{31}P NMR spectra of isolated perfused rat liver from a diabetic rat at 35 ± 1 °C. Spectrum a was measured 24–48 min after administration of 7.7 mM lactate. Spectrum b shows the same liver 12–36 min later and 12 min after administration of 7.7 mM pyruvate, 4.6 mM NH_4Cl, and 6.2 mM ethanol. Each spectrum is the accumulation of 1600 scans. Labeled peaks are as given in Figures 1 and 2 with the following exceptions: 3PG, 3-P-D-glycerate; X, unknown; A, dinucleotides; B, includes nucleoside diphospho sugars.

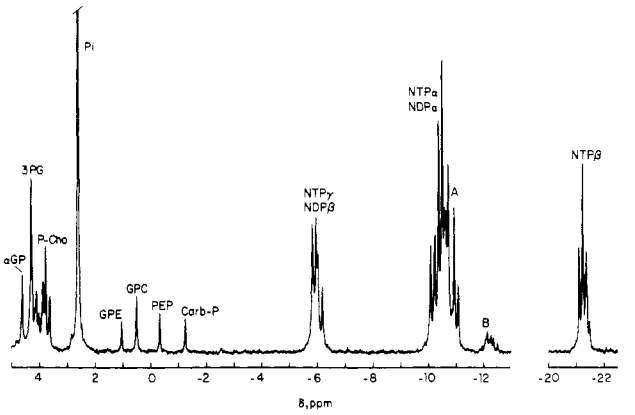

FIGURE 4: ^{31}P NMR spectrum of perchloric acid extract of freeze-clamped liver from diabetic rat at 12 °C. Shortly after the spectrum shown in Figure 3b was recorded, the liver was freeze-clamped and the extract shown here was prepared. Conditions are as given for Figure 2, except that here the pH was 7.8. Abbreviations are as given in Figure 3, with the addition that αGP = L-glycerol-3-P.

standard solutions (mitochondrial salt conditions) containing 3 mM carbamoyl-P at 35 °C, this chemical shift corresponded to a pH of about 6.6. However, when 4–5 mM Mg^{2+} was added to the standard solution and the pH was adjusted to 7.5, the chemical shift observed for carbamoyl-P in liver was reproduced.

^{13}C NMR Spectroscopy of Perfused Liver from Streptozotocin-Diabetic and Untreated Normal Rats. Figure 5 compares ^{13}C NMR spectra of perfused liver from a 24-h-fasted normal rat (Figure 5a) with liver from a diabetic rat (Figure 5b,c). Spectra a and c of Figure 5 contrast spectra of the normal and the diabetic liver at the *same* period of *time*

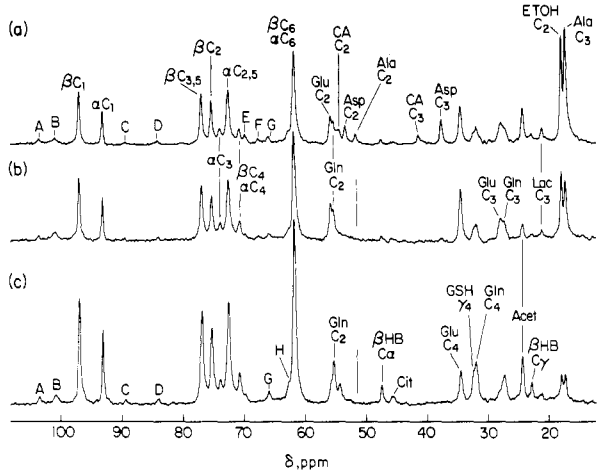

FIGURE 5: ^{13}C NMR spectra of isolated perfused livers from (a) normal, 24-h-fasted rat and (b and c) a diabetic rat at 35 ± 1 °C. Each spectrum is from a time sequence of spectra and represents 800 FIDs, acquired as described in the text. Spectrum a was measured 190–200 min after the initial addition of 10 mM [3-^{13}C]alanine and 7.3 mM [2-^{13}C]ethanol. Substrate was maintained close to this level by small, frequent (typically every 15 min) additions throughout the perfusion period. The ^{13}C natural abundance background spectrum of this liver was measured under identical conditions before substrate was added. For clarity of presentation, this background spectrum was subtracted from the spectrum shown. Spectra b and c are from a similar series of the same diabetic liver; spectra b and c were measured 110–120- and 190–200-min, respectively, postsubstrate. This diabetic liver was treated the same as the control liver in spectrum a. Spectra a and b represent comparison of control vs. diabetic for addition of the *same total quantity of substrate*, whereas spectra a and c represent comparison after the *same total time* of perfusion at approximately the same concentration of substrate. The labeled ^{13}C NMR peaks in these spectra include those due to the α and β anomers of D-glucose: βC-1, αC-1 to βC-6, αC-6. Other abbreviations include the following: Glu C_2, glutamate C-2; Gln C_2, glutamine C-2; Asp C_2, aspartate C-2; Ala C_2, alanine C-2; CA C_2, C-2 of *N*-carbamoylaspartate; GSHγ_4, C-4 of glutamyl moiety of reduced glutathione (overlaps C-4 of oxidized glutathione); Acet, C-2 of acetate; βHB Cα, C-2 of β-hydroxybutyrate; Cit, citrate CH_2; Lac C_3, lactate C-3; ETOH C_2, ethanol C-2. (A–E) See text; (F) 3-P-D-glucerate; (G) L-glycerol-3-P C-3; (H) C-1 and C-3 of glycerol (ester).

(190–200 min) after administration of [3-^{13}C]alanine and [2-^{13}C]ethanol. Spectra a and b of Figure 5, on the other hand, contrast spectra of the normal and diabetic liver at different periods of time after the initial administration of substrate but after addition of the *same* total *quantity* of *substrate*. (Steady-state conditions were approximated by maintaining substrate close to the initial level throughout the perfusion by the addition of small quantities of labeled alanine and ethanol to the perfusion reservoir at frequent intervals. Because of rapid consumption of substrate by diabetic liver, it was more difficult to keep levels constant throughout the accumulation of each spectrum of diabetic liver. However, levels of labeled substrates were monitored frequently during the measurement of each spectrum, so fluctuations were, in general of short duration.) In the low-field regions between 60 and 100 ppm, signals for newly synthesized, ^{13}C-labeled glucose are seen. Qualitatively, the ^{13}C enrichment in glucose is similar in both control (Figure 5a) and diabetic (Figure 5b,c) liver. In ^{13}C NMR spectra recorded before administration of ^{13}C-labeled substrate (not shown), no peaks due to the presence of glucose or glycogen with the 1.1% natural abundance of ^{13}C were detected. Comparison of the spectra in Figure 5 suggests that the rate of production of ^{13}C-labeled glucose from [3-^{13}C]-alanine was almost twice as great in the diabetic liver as in the liver from the 24-h-fasted normal rat. This suggestion is consistent with the greater consumption of ^{13}C-labeled substrate observed for diabetic liver. To test this possibility, aliquots (0.5 mL each) of perfusate were taken before the addition of substrate and at 40-min intervals, up to 200 min, throughout the perfusion of livers from diabetic and 24-h- or 12-h-fasted untreated rats. Perfusate erythrocytes were removed from the aliquots, and glucose concentrations were measured as described under Materials and Methods. These measurements provided the estimates of glucose synthesis given in Table I. The rates of glucose synthesis (in the absence of insulin) measured for liver from streptozotocin-treated and fasted untreated control rats are in general agreement with the relative intensities of the glucose resonances in the corresponding ^{13}C NMR spectra.

Table I: Glucose Synthesis in Isolated Perfused Liver from Streptozotocin-Diabetic and Untreated Control Rats[a]

donor rat	insulin	glucose synthesis [μmol (g of liver wet weight)$^{-1}$ h^{-1}]
diabetic (5)	–	51.7 ± 7.7
diabetic (4)	+	44.0 ± 12
24-h-fasted normal (4)	–	24.2 ± 4.3
24-h-fasted normal (3)	+	21.3 ± 3.4
12-h-fasted normal (3)	–	11.9 ± 1.6

[a] The substrates were either [3-^{13}C]alanine (10 mM) and [2-^{13}C]-ethanol (7.3 mM) or [2-^{13}C]pyruvate (9.1 mM), [2-^{13}C]ethanol (7.3 mM), and NH_4Cl (5.5 mM). Insulin, when added, was maintained at 7 nM. Rates of synthesis were calculated as described under Results. Rates were not corrected for the low glycolytic activity of the erythrocytes in the perfusate, which was measured in control studies (Cohen, 1983). Rates are given ± standard deviation for the number of experiments given within parentheses.

Flow of label is followed from [3-^{13}C]alanine into C-2, C-3, and C-4 of glutamate and glutamine in all three spectra in Figure 5. C-4 of glutamate and C-4 of glutamine are also traceable to [2-^{13}C]ethanol. Resonances assigned to C-2 and C-3 of aspartate, and to the corresponding carbons in *N*-carbamoylaspartate, are clearly seen in Figure 5a but not in Figure 5b,c. The resonance of the randomized C-2 of alanine is in evidence in Figure 5a but is not present at a detectable level in spectra of diabetic liver (vertical lines in Figure 5b,c) under these conditions. Variable levels of β-hydroxybutyrate are seen in all three spectra. The peaks labeled A, C, and D in Figure 5 are assigned to base C-5 and ribose moiety C-1 and C-4, respectively, of UTP, UMP, and uridine. Peak B is in the region of glycogen C-1 and CH_2 of PEP. Because a distinct signal from PEP is seen in ^{31}P NMR spectra of diabetic liver under these conditions (Figure 1b), it seems probable that PEP makes a significant contribution to the intensity of peak B in Figure 5b,c.

The three ^{13}C NMR spectra of a perfused diabetic liver shown in Figure 6 follow changes in concentrations of several metabolites over 10-min intervals commencing 10, 50, or 80 min after initial administration of [3-^{13}C]alanine. Clear signals from newly synthesized ^{13}C-labeled glucose are evident even 10-min postsubstrate and are seen to increase monotonically with time (Figure 6b,c). No ^{13}C enrichment is detectable in this diabetic liver at the randomized C-2 carbon of alanine under these conditions, even in the presence of relatively high levels of alanine with the original, unscrambled label at C-3. Glutamate C-2 and glutamine C-2, both of which can be traced directly back to the original label at C-3 of alanine, are more strongly labeled than glutamate C-3 and glutamine C-3. When the intensities are corrected for differences in NOE and T_1 (see Materials and Methods), the relative ^{13}C enrichments at glutamate C-2 and C-3 are in a ratio of about 70:30. In Figure 6c, a peak arising from glutathione labeled at γ-glu-

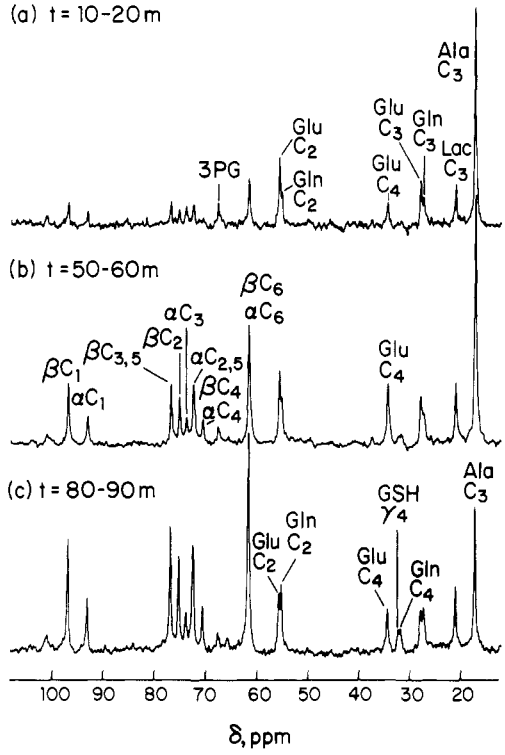

FIGURE 6: ^{13}C NMR spectra of perfused liver from a diabetic rat at 35 ± 1 °C. Spectrum a was measured 10–20 min after the addition of 10.0 mM [3-^{13}C]alanine, which was the only exogenous substrate present. Spectra b and c were accumulated during the period 50–60- and 80–90-min, respectively, postsubstrate. Other conditions and the abbreviations used are as given for Figure 5.

tamyl C-4 is resolved from a peak of about the same intensity arising from glutamine C-4. Label at glutamate C-4 was easily detected 10-min postsubstrate and achieved its steady-state level 20 min later. The ^{13}C enrichments at the corresponding carbons of glutamine and glutathione increased more slowly; these signals were only weakly detectable 1-h postsubstrate (Figure 6b) and reached their steady-state level 30 min later (Figure 6c).

The assignment of glutathione was aided by measurement of ^{13}C NMR spectra of perchloric acid extracts of livers freeze-clamped after perfusion under conditions known to introduce multiplet structure, due to ^{13}C–^{13}C scalar coupling, into the NMR peaks of precursor glutamate. The ^{13}C NMR peaks of the various metabolites are broadened in spectra of perfused liver (Figure 7a), whereas multiplet structure is resolved in spectra of the corresponding perchloric acid extracts (Figure 7b). The C-3 and C-4 resonances of glutamine and the γ-glutamyl moiety of glutathione show the same apparent triplet structure as C-3 and C-4, respectively, of precursor glutamate. These observations corroborate assignments based on chemical shift data. The outer doublet splittings measured at glutamate, glutamine, and glutathione, respectively, give values of 34.7, 35.0, and 34.8 Hz, respectively, for the coupling constant $J_{C3,C4}$.

It is well-known that the ^{13}C chemical shifts of the amino acids titrate with pH. Using standard solutions, we determined that over the pH range from 6.6 to 8.8 the signal of C-4 of the γ-glutamyl moiety of glutathione is clearly resolved from C-4 of glutamine, whereas the corresponding C-2 resonances overlap each other in the physiological pH range. The resonances of C-2 and C-3 of glutamine can be resolved from those of glutathione when the pH of the extract is adjusted to about 8.6 (expanded regions of Figure 7b). On the basis of the pH-dependent behavior of the ^{13}C chemical shifts of the γ-

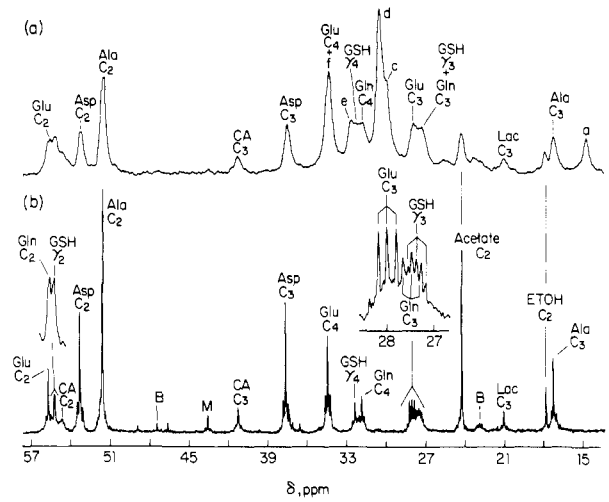

FIGURE 7: ^{13}C NMR spectra of perfused liver from a normal 12-h-fasted rat (a) and the perchloric acid extract of this liver (b). Spectrum a was accumulated 150–160 min after the addition of 9.1 mM [2-^{13}C]pyruvate, 5.5 mM NH_4Cl, and 7.3 mM [2-^{13}C]ethanol. Other conditions are as given for Figure 5. Shortly after spectrum a was recorded, the liver was freeze-clamped at the liquid nitrogen temperature and the extract shown in spectrum b was prepared. The pH of the extract was adjusted to 8.6. Spectrum b represents 9912 pulses of 30° FIDs, with a recycling time of 2.3 s at 12 °C. The regions between 17 and 57 pm, which contain several amino acid peaks, are shown. Abbreviations are as given in Figure 5, with the following exceptions: B, β-hydroxybutyrate; M, malate; a–f, see text.

glutamyl moieties of the reduced and oxidized forms of glutathione, GSH and GSSG, respectively, as compared with the corresponding chemical shifts of glutamine, the observable glutathione resonances in Figure 7b have been assigned to GSH. The parameter found to be most sensitive to pH was the chemical shift difference between C-2 of glutamine and C-2 of the γ-glutamyl moiety of either GSH or GSSG, denoted as Δ(Gln-GSH) or Δ(Gln-GSSG), respectively. Our assignment of GSH was made in the following way: (a) The C-2 resonances of glutamine and glutathione were not resolved in spectra of perchloric acid extracts of livers freeze-clamped after perfusion with either [2-^{13}C]pyruvate + NH_4Cl + ethanol or [3-^{13}C]alanine + ethanol, when the pH of the extract was 7.5–8.4 (n = four different extracts); however, at pH 8.60 (n = 2), Δ(Gln-glutathione) was 0.067 ppm, and at pH 8.65–8.85 (n = 7), Δ(Gln-glutathione) was 0.08 ppm. (b) To the perchloric acid extract of a liver that had been perfused with only unlabeled substrates, we added 15 mM authentic, unlabeled GSSG, 15 mM unlabeled glutamine, and 0.4 mM [3-^{13}C]-alanine as a reference standard. ^{13}C NMR spectra of this test extract, acquired under exactly the same conditions as were used for the ^{13}C-labeled extracts, showed that Δ(Gln-GSSG) increased smoothly with increasing pH. Δ(Gln-GSSG) was 0.060, 0.071, 0.081, 0.103, and 0.127 ppm at pH 7.95, 8.19, 8.36, 8.60, and 8.82, respectively. (c) To another perchloric acid extract of a liver perfused with only unlabeled substrates, we added 20 mM authentic, unlabeled GSH, 15 mM unlabeled glutamine, and 0.4 mM [3-^{13}C]alanine as reference. ^{13}C NMR spectra of this test extract showed that the C-2 resonances of glutamine and GSH were not resolved at pH 7.5–8.44. At pH 8.60, Δ(Gln-GSH) was 0.06 ppm, whereas at pH 8.70–8.82 Δ(Gln-GSH) was 0.08 ppm. These data suggest that the glutathione observed here in ^{13}C NMR spectra of perfused liver or the corresponding extracts exhibits pH-dependent behavior almost identical with that of authentic GSH but not at all like that of GSSG.

In general, ^{13}C NMR resonances were observed for C-2 and C-3 of the aspartate moiety of *N*-carbamoylaspartate when

Table II: ^{13}C NMR Measurement of Isotopic Distribution in Carbons of Glucose Formed from ^{13}C-Labeled Substrates by Isolated Perfused Liver from Streptozotocin-Diabetic Rats and from Fasted, Untreated Control Rats[a]

donor rat	substrate	relative ^{13}C enrichment of glucose						(C-1 + C-2 + C-3)/(C-4 + C-5 + C-6)
		C-1	C-2	C-3	C-4	C-5	C-6	
diabetic								
1	Ala[b,c]	95	79	22	19	83	100	0.97
2	Ala[b,c]	98	86	21	19	88	100	0.99
3	Ala[b]	96	80	25	21	81	100	1.00
4	Ala[b]	97	80	26	19	81	100	1.02
5	Ala[b]	99	84	20	16	84	100	1.02
6	Ala[b]	95	78	25	20	81	100	0.99
7	Ala[d]	100	84	36	34	82	100	1.02
8	Ala[c,d]	93	79	31	28	79	100	0.98
9	Pyr[b,e]	91	100	32	28	100	95	1.00
control								
1	Ala[b]	90	74	26	19	77	100	0.97
2	Ala[b]	92	74	21	15	76	100	0.98
3	Ala[b]	94	75	20	17	78	100	0.97
4	Ala[d]	87	74	37	39	87	100	0.88
5	Pyr[b,e]	82	89	36	34	100	96	0.90

[a] ^{13}C distributions are from the integrated intensities of the glucose lines in the NMR spectra of the perfusates recorded under nonsaturating conditions. The estimated error is ±2 units. Control rats 1–3 were fasted 24 h; controls 4 and 5 were fasted 12 h. Ala denotes 10 mM [3-^{13}C]-alanine, and Pyr denotes 9.1 mM [2-^{13}C]pyruvate. [b] Plus 7.3 mM [2-^{13}C]ethanol. [c] Insulin was maintained at 7 nM. [d] Plus 7.3 mM [1,2-^{13}C]ethanol. [e] Plus 5.5 mM NH_4Cl.

^{13}C-labeled aspartate was observed. The intensities of aspartate C-2 and C-3 in Figure 7b indicate equivalent ^{13}C enrichment at C-2 and C-3, within the estimated 5% error. As shown, the C-2 resonance of *N*-carbamoylaspartate was considerably broader than either of the aspartate peaks or the *N*-carbamoylaspartate C-3 resonance, even in perchloric acid extracts (Figure 7b). A similar broadening of the C-2 (but not the C-3) peak is observed in the ^{13}C NMR spectrum of authentic *N*-carbamoylaspartate (not shown). In addition to agreement of line widths and chemical shifts, the ^{13}C–^{1}H coupling constants measured at C-3 and C-2 of *N*-carbamoylaspartate in our perchloric acid extracts, 128.8 Hz and 140.6 Hz, respectively, agree with those measured for the authentic compound. From the aspartate C-3 outer doublet, $J_{C2,C3}$ = 36.0 Hz is measured; this splitting was not resolvable for *N*-carbamoylaspartate.

The five NMR peaks labeled a, c, d, e, and f in Figure 7a appear in spectra of perfused livers from 12-h-fasted rats but are not measured in spectra of the corresponding perchloric acid extracts (Figure 7b). In sharp contrast, these signals were not detected in spectra of liver from either streptozotocin-diabetic or 24-h-fasted rats (Figures 5 and 6). These five resonances have been assigned to carbons of fatty acyl chains produced in liver by de novo synthesis; specific assignments are given in a companion paper (Cohen, 1987b).

^{13}C NMR Spectroscopy of Perfusion Fluids. The metabolites detectable in ^{13}C NMR spectra of perfusion fluid at the termination of a perfusion of liver from a streptozotocin-diabetic rat are shown in Figure 8. Substrate was [3-^{13}C]alanine and [2-^{13}C]ethanol; insulin was maintained at 7 nM. Qualitatively, Figure 8 is representative of the metabolites measured in perfusion fluid following the perfusion of either control or diabetic liver. In general, strong signals were measured for glucose, lactate, and alanine; the signals of glutamine and glutamate were extremely weak. ^{13}C label was measurable at randomized carbons in alanine and lactate in the perfusion fluids for all control livers studied; label at these sites was observed in the case of normoxic diabetic liver only if insulin had been present during the perfusion. Even when appreciable signal was measured for glutathione in spectra of a perfused liver and its perchloric acid extract, glutathione was consistently below our level of detection (ca. 0.2 mM) in spectra of the corresponding perfusates.

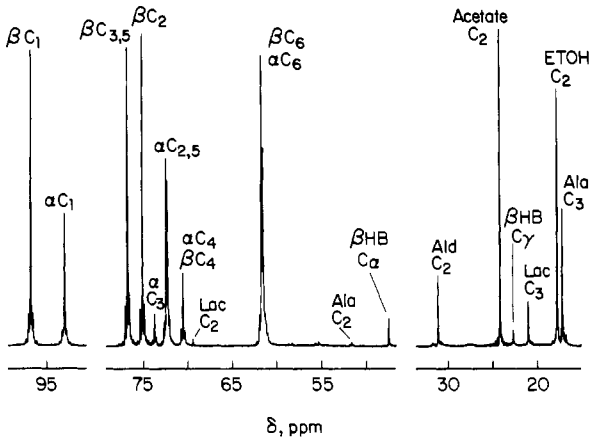

FIGURE 8: ^{13}C NMR spectrum of a perfusate measured subsequent to the perfusion of a liver from a diabetic rat. Substrate during the liver perfusion was 9.1 mM [3-^{13}C]alanine and 7.3 mM [2-^{13}C]ethanol; 7 nM insulin was added with the substrate. The erythrocytes were removed from the perfusate by centrifugation immediately upon termination of the perfusion. The region between 60 and 100 ppm contains the glucose peaks. The spectrum is the Fourier transform of the accumulation of 3600 pulses of 30° free induction decays, with 3.5-s recovery between pulses. The abbreviations are as given in Figures 5 and 7, except that Ald C_2 is C-2 of acetaldehyde.

Strong and roughly equal labeling of carbons 1, 2, 5, and 6 was observed in glucose synthesized by liver under our conditions (Figure 8). The anomers of glucose are known to be in equilibrium, and from the integrated intensities of the C-1 peaks, the ratio of β to α anomer was typically 63:37. The data in Table II show the relative ^{13}C enrichment at the carbons of glucose for nine diabetic livers and five control livers.

The metabolism of labeled ethanol is conveniently monitored in ^{13}C NMR spectra of the perfusion fluids. When ^{13}C-labeled ethanol was administered with the gluconeogenic substrate, signals for acetate, acetaldehyde and β-hydroxybutyrate were seen (Figure 8). No acetoacetate was detected in perfusate under these same conditions (n = 11). ^{13}C NMR spectra of the perfusates and the data in Table II provide sufficient information to calculate the rate of oxidation of ethanol, the amount of acetaldehyde, produced from labeled ethanol, that left the liver unmetabolized, and the concentration of acetate that accumulated in the perfusion fluid. These estimates were

Table III: ^{13}C NMR Measurement of Metabolism of ^{13}C-Labeled Ethanol by Perfused Liver from Streptozotocin-Diabetic Rats and Fasted, Untreated Control Rats[a]

donor rat	substrate	μmol (g of liver wet weight)$^{-1}$ min^{-1}			acetaldehyde not further metabolized	acetate as % of ethanol oxidized
		ethanol oxidized	acetaldehyde output	acetate accumulation		
diabetic						
1	Ala[b,c]	1.28	0.10	0.51	7.8	40
2	Ala[b,c]	1.43	0.13	0.78	9.1	55
3	Ala[b]	0.98	0.02	0.10	2.0	10
4	Ala[b]	1.19	0.09	0.62	7.6	52
5	Ala[b]	1.49	0.02	0.37	1.3	25
6	Ala[b]	1.01	0.03	0.18	3.0	18
7	Ala[d]	1.20	0.09	0.48	7.5	40
8	Ala[c,d]	0.96	0.02	0.24	2.5	25
9	Pyr[b,e]	1.68	0.03	0.22	1.8	13
control						
1	Ala[b]	0.49	0.05	0.44	10.0	85
2	Ala[b]	1.42	0.03	0.69	2.1	49
3	Ala[d]	1.25	0.03	0.34	2.6	27
4	Pyr[b,e]	1.49	0.02	0.50	1.1	34

[a] Concentrations of the metabolites were measured in the perfusates of 13 perfused rat livers by ^{13}C NMR as described in the text. The estimated error is ±9%. Ala denotes 10 mM [3-^{13}C]alanine, and Pyr denotes [2-^{13}C]pyruvate. [b] Plus 7.3 mM [2-^{13}C]ethanol. [c] Insulin was maintained at 7 nM. [d] Plus 7.3 mM [1,2-^{13}C]ethanol. [e] Plus 5.5 mM NH_4Cl.

made in the following way: (a) The concentration of glucose in the perfusates was determined as described above. (b) The ^{13}C enrichment at glucose C-6 was calculated in absolute terms from the total concentration of glucose and the relative ^{13}C enrichments (Table II) with a first-order approach (Cohen, 1983). Relative enrichments were confirmed by ^1H NMR. (c) The integrated intensities of the peaks due to ethanol, β-hydroxybutyrate, acetate, acetaldehyde, and glucose C-6 in the ^{13}C NMR spectra of the perfusates, with application of the appropriate correction factors for NOE and T_1 effects (see Material and Methods), were then used to calculate the absolute rates given in Table III. It is important to note that in perfusions when unlabeled, rather than ^{13}C-labeled, ethanol was administered, no signal from either acetate or acetaldehyde was detected in spectra of the perfusates (not shown). In four out of nine experiments using liver from diabetic rats, more than 7% of the acetaldehyde produced from ethanol left the liver unmetabolized; in only one out of four experiments using normal liver was this the case. With one exception, from 40 to 90% of the acetate produced was further metabolized by the liver. Using this same approach, we estimated that β-hydroxybutyrate production was 7.0 ± 2.0 and 4.6 ± 1.4 μmol (100 g of body weight)$^{-1}$ h^{-1} in diabetic (n = 7) and control (n = 4) liver, respectively.

Discussion

^{31}P NMR. ^{31}P and ^{13}C NMR were used to compare the metabolism of ^{13}C-labeled gluconeogenic substrates in perfused liver from streptozotocin-diabetic rats and their untreated littermates. Because ^{31}P and ^{13}C chemical shifts are, in general, fairly specific, it was possible to distinguish and measure a large number of metabolites in a single spectrum. Although it could not have been anticipated, appreciable signal from an unusual P,P′-diesterified pyrophosphate was detected in the ^{31}P NMR spectra of 25% of the diabetic livers examined. This metabolite was not observed in the rest of the diabetic livers or in any control liver. While it has not yet been identified, this metabolite is clearly not one of the compounds of this general type usually found in liver. The toxicity of streptozotocin correlates with short-term depression of NAD^+ and is prevented by coadministration of nicotinamide (Schein et al., 1967). The appearance of the unusual NAD^+ analogue in the ^{31}P spectra may possibly be related to this toxicity.

Carbamoyl phosphate was measured in ^{31}P NMR spectra of all diabetic livers but not in spectra of any control liver under our conditions. Meijer et al. (1985) have provided strong evidence showing that essentially all the carbamoyl-P present in rat liver resides in the mitochondria. With the assumption that this condition obtains under our conditions and with use of the mitochondrial to cytosolic volume ratio calculated by Tischler et al. (1977), the intramitochondrial carbamoyl-P level is estimated to be about 4 mM in diabetic liver (Figure 3b). This value agrees well with the intramitochondrial level measured by Meijer et al. (1985) in hepatocytes from normal rats incubated under conditions when ornithine was limited but intracellular levels of amino acids were high. Carbamoyl-P thus appears to be a reliable intramitochondrial marker in ^{31}P NMR spectra. It seems probable that (1) carbamoyl-P observed here in spectra of diabetic liver was synthesized by the mitochondrial carbamoyl-P synthetase for ureogenesis and (2) its appearance indicates that the synthesis of urea was ornithine-limited in diabetic liver but not in control liver. The chemical shift of carbamoyl-P in liver was reproduced in model solutions when Mg^{2+} was added and the pH adjusted to 7.5, which is the pH usually estimated for mitochondria (Rottenberg, 1975). Consistent with our observations, a peak measured at about the same chemical shift in ^{31}P NMR spectra of isolated rat liver mitochondria has been tentatively identified as carbamoyl-P (Ogawa & Lee, 1982). Because carbamoyl-P shows weak binding to Mg^{2+} and because of the many variables capable of affecting ^{31}P chemical shifts in mitochondria, use of this marker to estimate the mitochondrial free Mg^{2+} level was not pursued.

^{13}C NMR. The major gluconeogenic pathway from labeled alanine or labeled pyruvate was followed by ^{13}C NMR. Endogenous glycogen levels are known to be low in diabetic liver (Exton et al., 1973), and in normal liver glycogen levels are almost as low after a 12-h fast as after a 24-h fast (Solling et al., 1973). Thus, both the preparation of the animals and the lengthy period of preliminary nonrecirculating perfusion in the absence of substrate used here tended to minimize contributions from unlabeled sources. For these reasons, it seems reasonable to assume that, to a good approximation, glucose present in the liver and perfusate under our conditions was ^{13}C-labeled and was synthesized from the ^{13}C-labeled substrates. As suggested by comparison of ^{13}C NMR spectra of diabetic and control liver (Figure 5), the rate of gluconeogenesis measured for diabetic liver was 2-fold and 4-fold

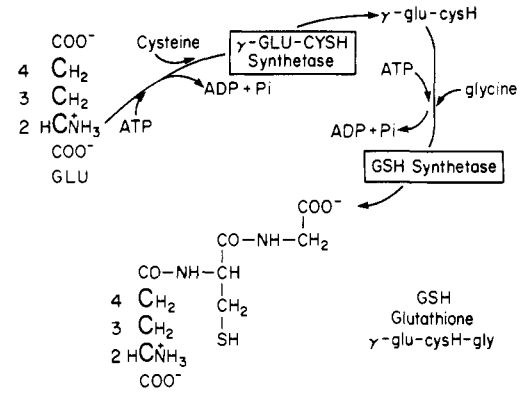

FIGURE 9: Simplified model pathway for synthesis of ^{13}C-labeled glutathione from ^{13}C-labeled glutamate.

greater than the rates measured for 24-h- and 12-h-fasted controls, respectively (Table I). Rates of gluconeogenesis measured here are comparable to rates measured previously in liver from alloxan-diabetic and normal control rats (Exton et al., 1972, 1973).

By the approach used here, two important metabolites, glutathione and *N*-carbamoylaspartate, which had not been assigned in our previous ^{13}C NMR studies, were observed and identified.

N-Carbamoylaspartate is produced in liver in the second step of the de novo pathway of pyrimidine nucleotide synthesis. *N*-Carbamoylaspartate incorporates the intact aspartate moiety. Thus, as would be anticipated, ^{13}C enrichments observed in liver at aspartate C-2 and C-3 were also observed at the corresponding positions in *N*-carbamoylaspartate. This correlation is compatible with a report that suggests a potential regulatory role for cytosolic aspartate in hepatic de novo pyrimidine synthesis (Pausch et al., 1985). Appearance of ^{13}C label in the pathway end products, such as uridine, UMP, and UTP (Figure 5), in ^{13}C NMR spectra of diabetic and control liver suggests that true synthesis of *N*-carbamoylaspartate, as opposed to turnover, was followed. Consonant with this suggestion, the equilibrium of the aspartate transcarbamoylase catalyzed reaction is strongly in favor of synthesis of *N*-carbamoylaspartate (White et al., 1978). ^{13}C-Labeled pyrimidine production was observed in diabetic liver in the absence of detectable levels of *N*-carbamoylaspartate (Figure 5c). A resonable explanation for this production is provided by recent results showing that mitochondrial carbamoyl phosphate accumulation—which was observed here in diabetic liver—can lead to a stimulation of pyrimidine synthesis (Pausch et al., 1985).

The multiple roles of glutathione in liver are well recognized (Meister & Anderson, 1983). Appreciable levels of glutathione were observed in ^{13}C NMR spectra of both normal control liver and diabetic liver (Figures 5–7). This observation is consistent with reports that the total quantity of glutathione in rat liver is in the millimolar range, while lack of signal from glutathione in the perfusion fluid (Figure 8) is consistent with a micromolar range for plasma glutathione (Kosower & Kosower, 1978). The ^{13}C NMR observable glutathione resonances in liver were assigned to the reduced form, GSH, on the basis of ^{13}C NMR studies of perchloric acid extracts of the freeze-clamped livers. This assignment is compatible with the ratio of 300:1 measured by Ackerboom et al. (1982) for GSH/GSSG in perfused liver from fed rats. Large perturbations of the normal intracellular glutathione redox state are not expected under our perfusion conditions. As shown in Figure 9, glutathione incorporates the glutamate moiety intact. Thus, the same multiplet structure, due to ^{13}C–^{13}C scalar coupling, should be observed in the NMR peaks of corresponding carbons of glutamate and glutathione and, of course, also glutamine. This expectation was confirmed in spectra of the perchloric acid extracts of the freeze-clamped livers (Figure 7). Both C-3 and C-4 are labeled in the *same* molecule of glutamate in a significant fraction of the glutamate pool in liver incubated with [2-^{13}C]pyruvate, NH_4Cl, and [2-^{13}C]ethanol (Cohen, 1983). In this circumstance, the NMR resonances of glutamate C-3 and C-4 each consist of an apparent triplet, with the outer doublet arising from carbon–carbon *J* coupling between ^{13}C-3 and ^{13}C-4 and the center singlet due to ^{13}C-3(4) residing next to unlabeled C-4(3). To a first approximation, C-2 and C-3 are not both labeled in the same molecule of glutamate. The signals of C-2, C-3, and C-4 of glutamate in Figure 7b are consistent with these predictions. In perfused liver the C-2 and C-3 signals of the γ-glutamyl moiety of glutathione were not resolved from signals for the corresponding carbons of glutamine. However, observation of the γ-glutamyl C-4 peak, which was resolved, strongly suggests that the peaks labeled, for convenience, simply Gln C_2 or Gln C_3 in spectra of perfused liver, such as Figure 6, include contributions from glutathione. A lower limit on these contributions can be estimated from the ^{13}C enrichment at γ-glutamyl C-4 of glutathione relative to glutamate C-4 and from the relative enrichments of glutamate C-2 and C-3. Synthesis of glutathione labeled at C-4 was observed to lag behind that of glutamate labeled at C-4 by at least 1 h (Figure 6). Glutathione undergoes continuous turnover, with a biological half-life in the range of 2–4 h in rat liver (Kosower & Kosower, 1978). The biosynthesis of GSH appears to be rate limited by the availability of intracellular cysteine (Tateishi et al., 1974) (Figure 9). It seems possible that cysteine-limited conditions caused the delay in GSH synthesis measured here. That is, synthesis of GSH with a labeled γ-glutamyl moiety could not begin until cysteine had been released from endogenous GSH via normal turnover (Meister & Anderson, 1983).

^{13}C NMR of Perfusion Fluids. The relative ^{13}C enrichments at the carbons of glucose measured in spectra of perfusion fluids (Table II) are useful in several applications. (1) The ^{13}C enrichments in glucose C-4, C-5, and C-6 reflect the labeling of cytosolic oxalacetate and are useful in quantitative estimates of metabolic fluxes (Cohen, 1987a). (2) The ^{13}C enrichments in glucose, together with measurements of glucose concentrations in aliquots of perfusate taken at time intervals, allowed us here to use glucose as a convenient internal concentration standard for ^{13}C NMR spectra of perfused liver or perfusate. (3) Modification and loss of ^{13}C label in glucose C-1, C-2, and C-3 are usually considered to be indicative of pentose cycle activity (Cohen et al., 1981b). Thus, the ratios of glucose (C-1 + C-2 + C-3)/(C-4 + C-5 + C-6) of about 1.0 measured for liver from diabetic or 24-h-fasted rats (Table II) suggest that pentose cycle activity was very low in these livers. The lower ratios measured for liver from 12-h-fasted rats (controls 4 and 5, Table II) suggest a more active pentose cycle and are consistent with the evidence of de novo synthesis of fatty acids mentioned above. (4) The greater labeling of glucose C-3 and C-4 measured when either [1,2-^{13}C]ethanol or [2-^{13}C]pyruvate (both of which produce acetyl-CoA labeled at carbon 1) was present during the incubation is consistent with a previous analysis of TCA cycle fluxes (Cohen, 1983).

^{13}C NMR analysis of the perfusion fluids provided rapid, simultaneous assays of the rates of oxidation of [^{13}C]ethanol, the output of [^{13}C]acetaldehyde from the liver, and the accumulation of [^{13}C]acetate in the perfusate (Table III). The metabolism of ethanol in experimental diabetes does not appear

to have been investigated before. With one exception, the rate of oxidation of 7 mM ethanol was not significantly different in diabetic and control liver. The average rate of ethanol oxidation measured here is about 2-fold lower than the rate typically observed for liver from fasted normal rats during incubations with similar substrates (Braggins et al., 1980; Williamson & Tischler, 1979). Use of ^{13}C-labeled ethanol is not expected to introduce a significant isotope effect. Strain differences may account for the different rates of oxidation of ethanol measured in these various studies.

^{13}C NMR spectra of the perfusion fluids (Figure 8) measure the amount of [^{13}C]acetaldehyde that was produced by action of liver alcohol dehydrogenase on [^{13}C]ethanol and which subsequently left the liver before being oxidized to acetate. The highest output of acetaldehyde observed here during the oxidation of 7 mM ethanol is about one-third of the maximum output measured by Braggins et al. (1980) during the oxidation of 32 mM ethanol by perfused liver. In general, liver is considered to be capable of metabolizing approximately 90–95% of the acetaldehyde produced during ethanol oxidation (Weiner, 1979). Accordingly, in all perfusions listed in Table III, 10% or less of the acetaldehyde produced left the liver without being further metabolized. In contrast, Williamson et al. (1969) found only trace amounts of acetaldehyde released by perfused liver. The mechanism responsible for these differences is obscure but may be related to the use of erythrocytes in the perfusion fluid in this study and by Braggins et al. (1980) but not by Williamson et al. (1969). That is, the ability of acetaldehyde to react with hemoglobin and other proteins by adduct formation (Stevens et al., 1981) may provide a reasonable explanation for the increased output of acetaldehyde by liver perfused with medium containing erythrocytes.

Treatment of rats with streptozotocin at the dose level used here (45 mg/kg) produces an essentially nonketotic form of diabetes, whereas treatment at higher dose levels produced the ketotic form of diabetes (Schein et al., 1971). Both [3-^{13}C]alanine and [2-^{13}C]ethanol enter the mitochondrial acetyl-CoA pool as [2-^{13}C]acetyl-CoA, which in turn forms ketone bodies labeled at C-2 and C-4. ^{13}C-labeled β-hydroxybutyrate was observed in perfused liver (Figure 5) and, more conveniently, in the perfusion fluid (Figure 8). Although inter-liver variations are seen, in ^{13}C NMR spectra of the perfusates an average increase of 50% in β-hydroxybutyrate production was measured for diabetic liver, which agrees well with the increase measured previously in liver from rats treated with streptozotocin at almost the same dose level, whereas triplet this dose caused a 5-fold increase in β-hydroxybutyrate (Schein et al., 1971).

In conclusion, both ^{13}C and ^{31}P NMR are useful in defining the changes in hepatic metabolism that occur in the streptozotocin-diabetic rat and together can provide a wide range of detailed biochemical information. By the approach used here it was possible to determine the metabolic fate of several substances simultaneously.

ACKNOWLEDGMENTS

I am grateful to Richard Saperstein and E. W. Chapin for the streptozotocin-treated rats, to MaryLou James for technical assistance, to Shirley Satiritz for the glucose assays, and to Stacianne Fischbach for typing the manuscript.

Registry No. ATP, 56-65-5; P_i, 14265-44-2; UTP, 63-39-8; UMP, 58-97-9; PEP, 138-08-9; GSH, 70-18-8; GSSG, 27025-41-8; insulin, 9004-10-8; carbamoyl phosphate, 590-55-6; alanine, 56-41-7; pyruvate, 127-17-3; ethanol, 64-17-5; glycogen, 9005-79-2; glutamate, 56-86-0; glutamine, 56-85-9; aspartate, 56-84-8; β-hydroxybutyrate, 300-85-6; uridine, 58-96-8; lactate, 50-21-5; acetate, 64-19-7; acetaldehyde, 75-07-0.

REFERENCES

Ackerboom, T. P. M., Bilzer, M., & Sies, H. (1982) *J. Biol. Chem. 257*, 4248–4252.

Braggins, T. J., Crow, K. W., & Batt, R. D. (1980) in *Alcohol and Aldehyde Metabolizing Systems* (Thurman, R. G., Ed.) Vol. 4, pp 441–449, Plenum, New York.

Canet, D. (1976) *J. Magn. Reson. 23*, 361–364.

Cohen, S. M. (1983) *J. Biol. Chem. 258*, 14294–14308.

Cohen, S. M. (1987a) *Biochemistry* (second paper of three in this issue).

Cohen, S. M. (1987b) *Biochemistry* (third paper of three in this issue).

Cohen, S. M., Glynn, P., & Shulman, R. G. (1981a) *Proc. Natl. Acad. Sci. U.S.A. 78*, 60–64.

Cohen, S. M., Rognstad, R., Shulman, R. G., & Katz, J. (1981b) *J. Biol. Chem. 256*, 3428–3432.

Exton, J. H., Corbin, J. G., & Harper, S. C. (1972) *J. Biol. Chem. 247*, 4996–5003.

Exton, J. H., Harper, S. C., Tucker, A. L., & Ho, R.-J. (1973) *Biochim. Biophys. Acta 329*, 23–40.

Kosower, N. S., & Kosower, E. M. (1978) *Int. Rev. Cytol. 54*, 109–160.

Kraus-Friedmann, N. (1984) *Physiol. Rev. 64*, 170–259.

Meijer, A. J., Lof, C., Ramos, I. C., & Verhoeven, A. J. (1985) *Eur. J. Biochem. 148*, 189–196.

Meister, A., & Anderson, M. E. (1983) *Annu. Rev. Biochem. 52*, 711–760.

Ogawa, S., & Lee, T.-M. (1982) *Biochemistry 21*, 4467–4473.

Pausch, J., Rasenack, J., Haussinger, D., & Gerok, W. (1985) *Eur. J. Biochem. 150*, 189–194.

Pople, J. A., Schneider, W. G., & Bernstein, H. J. (1959) *High-Resolution Nuclear Magnetic Resonance*, Chapter 6, McGraw-Hill, New York.

Rottenberg, H. (1975) *Bioenergetics 7*, 61–74.

Schein, P. S., Cooney, D. A., & Vernon, M. L. (1967) *Cancer Res. 27*, 2324–2332.

Schein, P. S., Alberti, K. G. M. M., & Williamson, D. H. (1971) *Endocrinology (Philadelphia) 89*, 827–834.

Schwenke, W.-D., Soboll, S., Seitz, H. J., & Sies, H. (1981) *Biochem. J. 200*, 405–408.

Solling, H. D., Kleineke, J., Willms, B., Janson, G., & Kuhn, A. (1973) *Eur. J. Biochem. 37*, 233–243.

Stevens, V. J., Fantl, W. J., Newman, C. B., Sims, S. V., Cerami, A., & Peterson, C. M. (1981) *J. Clin. Invest. 67*, 361–369.

Tateishi, N., Higashi, T., Shinyz, S., Naruse, A., & Sakamoto, Y. (1974) *J. Biochem. (Tokyo) 75*, 93–103.

Tischler, M. E., Hecht, P., & Williamson, J. R. (1977) *Arch. Biochem. Biophys. 181*, 278–292.

Weiner, H. (1979) in *Biochemistry and Pharmacology of Ethanol* (Majchrowicz, E., & Noble, E. P., Eds.) Vol. 1, pp 125–144, Plenum, New York.

White, A., Handler, P., Smith, E. L., Hill, R. L., & Lehman, R. I. (1978) *Principles of Biochemistry*, p 765, McGraw-Hill, New York.

Williamson, J. R., & Tischler, M. (1979) in *Biochemitry and Pharmacology of Ethanol* (Majchrowicz, E., & Noble, E. P., Eds.) Vol. 1, pp 167–189, Plenum, New York.

Williamson, J. R., Scholz, R., Browning, E. T., & Thurman, R. G. (1969) *J. Biol. Chem. 244*, 5044–5054.